2025 IEEE 21st International Conference on Automation Science and Engineering (CASE)
August 17-21, 2025. Los Angeles, CA, US

2025 IEEE 21st International Conference on Automation Science and Engineering (CASE) | 979-8-3315-2246-9/25/$31.00 ©2025 IEEE | DOI: 10.1109/CASE58245.2025.11164150

Hybrid Control for Robot Swarms to Detect Critical Nodes in Heterogeneous Sensor Networks

Yun Gao, Ziai Zhou, Hao Gao, Shiheng Zhang, and Yiding Ji†

***Abstract*— Robot swarms have recently shown great promise in monitoring the operation of heterogeneous sensor networks (HSNs). However, current methods suffer from prohibitive search costs and inaccurate detection of critical nodes that require maintenance. In this study, we develop a hybrid control approach that integrates two control stages to efficiently identify maintenance-requiring nodes within a widely deployed HSN using robot swarms, providing reliable support for subsequent maintenance tasks. First, we introduce a coverage control strategy based on the Voronoi tessellation of the task environment, rapidly identifying areas with high signal intensity (SI) in the HSN. Next, we define the Node Influence metric to quantitatively measure the urgency of maintenance for each node based on SI and the robustness of the connections between nodes. Then, we switch to another control profile to identify nodes that potentially require maintenance. We also prove the convergence and correctness of the method. Finally, results from numerical simulation and experiments are provided to validate the efficiency, scalability, and transferability of our approach.**

***Index Terms*— Robot swarms, node detection, hybrid control, coverage control, heterogeneous sensor networks.**

I. Introduction

Monitoring complex environments requires a variety of sensors, and the advance of multi-sensor fusion technology enables different types of sensors to collaborate and form heterogeneous sensor networks (HSNs) [1], [2]. HSNs are increasingly prevalent in real-world applications involving intricate tasks, such as search and rescue operations, logistics distribution, and environmental governance [3]–[5]. However, sensors deployed in the environment may deviate from their original positions due to vibrations, impacts, and other factors, leading to changes in the network topology. Such topological variations may result in a shift in the structural importance of certain nodes that are essential for maintaining the connectivity of HSNs. In this study, we refer to these nodes, whose importance emerges from the evolving topology itself, as maintenance-requiring nodes (MRNs).

When HSNs experience failures or performance degradation, the original role assignments based on initial deployment configurations often become obsolete, rendering maintenance strategies derived from them ineffective. Consequently, it becomes imperative to identify the nodes that have become critical in the new topology to ensure the stability and continued functionality of HSNs [6].

Although the MRNs are inherently dynamic, the standard for their evaluation should remain consistent. Therefore, the first challenge is to develop a robust and unified evaluation standard to accurately determine whether a node needs maintenance. Some common metrics defined from network theory, such as degree centrality, betweenness centrality, and eigenvector centrality [7], have inherent limitations: they are not suitable for sparse networks or networks with a large diameter [8], and incur a high computational cost in large-scale networks [9]. Although some new metrics, such as vulnerability level [10], have recently been proposed to define MRNs, they often do not accurately reflect the robustness of connections between nodes in weighted networks. Specifically, nodes with the same vulnerability level may be located at either the network's core or periphery, which will mislead the robots and cause unsuccessful detection [11].

The second challenge is that if a large-scale HSW is deployed over a large area, manual inspection of thousands of nodes is impractical. To address this challenge, deploying a robot swarm (RS) to systematically explore the task area and collect comprehensive information from all nodes for evaluation represents a promising and effective approach [12]–[15]. RSs implement distributed control strategies that enable efficient inspection of numerous nodes, facilitating node detection through a divide-and-conquer approach [16], [17].

Various spatial partitioning methods have been proposed to achieve target coverage in the field of RSs [18], [19]. However, these methods tend to be inefficient as the scale of the network increases. Furthermore, many detection schemes require prior knowledge of the HSNs, such as network topology or node kinematics [20], which may not be feasible in certain scenarios. For instance, if urban base stations are damaged after an earthquake, the information of their location, coverage, and connectivity may be dramatically altered, rendering prior knowledge irrelevant [21]. The urgency of rescue operations often makes it impractical for RSs to traverse all targets for MRN detection.

In light of these challenges, this work focuses on identifying nodes within HSNs that exhibit high signal intensity (SI) but low connection robustness, as failures in these nodes could lead to widespread network disconnections. We propose a two-stage distributed control framework for efficiently identifying MRNs in HSNs using RSs. In the first stage, we introduce a coverage control technique based

Y. Gao, H. Gao, S. Zhang, and Y. Ji are with Robotics and Autonomous Systems Thrust, Hong Kong University of Science and Technology (Guangzhou), Guangzhou, China. (Emails: y.gao@gaoyunailab.com, florianzsh7@gmail.com, ghalfred39@gmail.com, jiyiding@hkust-gz.edu.cn.)

Z. Zhou is with School of Information Science and Engineering, Shandong University, Jinan, China. (Email: 202000210104@mail.sdu.edu.cn.)

†Corresponding author.

Financial support: National Natural Science Foundation of China grants 62303389, 62373289; Guangdong Basic and Applied Basic Research Funding grants 2022A151511076, 2024A1515012586; Guangdong Scientific Research Platform and Project Scheme grant 2024KTSCX039; Guangzhou-HKUST(GZ) Joint Funding Program grants 2024A03J0618, 2024A03J0680.

on Voronoi tessellation to effectively distribute the robots across the target area. Subsequently, a gradient-based control profile is implemented for the RSs to locate target areas based on SI. In the second stage, the RS evaluates the Node Influence (NI) of each node using onboard detection devices, employing global coordination to pinpoint the MRNs. The main contributions of this paper are summarized as follows:

- We develop an innovative hybrid control scheme for RSs to explore HSNs and detect nodes requiring maintenance;
- we propose a two-stage strategy for area exploration followed by node detection, which outperforms conventional coverage control and exhaustive detection methods. Our method significantly improves node identification speed and efficiency, without prior information about HSNs;
- We introduce a novel metric NI to quantitatively assess the urgency of maintenance for each node based on SI of the HSN and the strength of node connections. Compared to existing metrics, NI significantly improves detection accuracy and is more applicable in various scenarios.

The remainder of this paper is organized as follows. Section II models the RSs and HSNs, then formulates the key problem. Section III details the solution procedure comprising a two-stage hybrid control strategy, then briefly analyzes the correctness of the proposed method. Section IV presents simulation results that demonstrate the practical performance of our approach. Finally, Section V concludes the paper and outlines several future research directions.

II. Preliminaries and Problem Formulation

Consider an RS with I identical robots, indexed by $\{1, 2, \ldots, I\}$, moving in a two-dimensional convex and compact plane $\mathcal{Q} \subset \mathbb{R}^2$. Let $p_i^{\mathrm{r}}(k) \in \mathbb{R}^2$ denote the location of the i^{th} robot at time k. The instantaneous configuration of the RS is $P^{\mathrm{r}}(k) = [p_1^{\mathrm{r}}(k), \ldots, p_i^{\mathrm{r}}(k), \ldots, p_I^{\mathrm{r}}(k)]$. The position of the i^{th} robot follows the first-order model:

$$p_i^{\mathrm{r}}(k+1) = p_i^{\mathrm{r}}(k) + T_s u_i(k), \tag{1}$$

where $u_i(k)$ is the control input at time k, $u_i(k) \leq v$ represents the control bound, $v \in \mathbb{R}_{>0}$ is the maximum linear velocity of the robot, and T_s is the sample time.

Robots communicate with each other within a circular area of radius $R_c \in \mathbb{R}_{>0}$. We apply Euclidean distance to measure the distance between two points in $\mathcal{Q}$. For the i^{th} and j^{th} robots, $\left\|p_i^{\mathrm{r}}(k) - p_j^{\mathrm{r}}(k)\right\| \leq R_c$ represents a bidirectional communication link within their communication range.

Robots are also capable of detecting sensors within a disk of radius $R_d \in \mathbb{R}_{>0}$, acquiring information on positions, neighboring nodes and the environment. The perception capacity decreases as the distance between robots and sensors increases, which follows the differentiable function below:

$$f(q, p_i^{\mathrm{r}}(k)) = \begin{cases} \delta e^{-\lambda \|q - p_i^{\mathrm{r}}(k)\|^2} - \alpha & \|q - p_i^{\mathrm{r}}(k)\| \leq R_d, \\ 0 & \|q - p_i^{\mathrm{r}}(k)\| > R_d, \end{cases} \tag{2}$$

where $q \in \mathcal{Q}$ is at any point within the task area, $\delta \in (0, 1)$ is a coefficient representing the maximum perceptual ability, $\lambda \in (0, \infty)$ is the attenuation coefficient, and $\alpha = \delta e^{-\lambda R_d^2}$ is a constant that returns the boundary to zero.

Given a plane $\mathcal{Q} \subset \mathbb{R}^2$, an HSW consists of N sensors that may exchange information with each other through the wireless module they assembled and have different communication capacities. We employ the Gaussian function, represented as $g(q, p_n^{\mathrm{s}}) = \exp(-\frac{1}{2\sigma_n^2} \|q - p_n^{\mathrm{s}}\|^2)$, to describe the signal intensity (SI) among the sensors, where σ_n is the speed of SI attenuation that determines the sensing range and $p_n^{\mathrm{s}} \in \mathcal{Q}$ is the position of the n^{th} sensor in the HSN. This allows us to view $\mathcal{Q}$ as a non-uniform SI field and compute the SI at any q as $\phi(q) = \sum_{n=1}^{N} \gamma_n g(q, p_n^{\mathrm{s}})$, where γ_n is the heterogeneous feature parameter for the n^{th} sensor. The adoption of HSWs setting, where sensors differ in both SI and sensing ranges, not only aligns with the variability commonly observed in real-world sensor deployments but also enhances the generality of our model. Thus, our proposed framework not only applies to idealized homogeneous networks but to a broader range of practical scenarios.

Formally, an HSN is abstracted as an undirected graph $\mathcal{G} = (\mathcal{V}, \mathcal{E})$ where $\mathcal{V} = \{1, 2, \ldots, N\}$ denotes the set of vertices and $\mathcal{E} \subseteq \mathcal{V} \times \mathcal{V}$ denotes the set of edges. Several notions are defined to capture the properties of HSNs.

Definition 1 (Path)**.** *Given $\mathcal{G}$, a path between the n^{th} and m^{th} node, denoted by $\pi(n, m)$, is a sequence of vertices where there is an edge between every two adjacent vertices. We denote by $\Pi(n, m)$ the set of all paths between the n^{th} and m^{th} node. With a slight abuse of notations, we also denote by $\Pi(n, S) = \bigcup_{m \in S} \Pi(n, m)$ as the set of all paths between the n^{th} node and a set of nodes $S \subseteq \mathcal{V}$ in $\mathcal{G}$.*

Definition 2 (Path length)**.** *The length of a path $\pi(n, m)$ is the number of its edges, denoted by $|\pi(n, m)|$.*

Definition 3 (Communication distance)**.** *The communication distance between the n^{th} and m^{th} node in $\mathcal{G}$ is defined as $d(n, m) = \min_{\pi(n,m) \in \Pi(n,m)} |\pi(n, m)|$.*

Definition 4 (Neighbors)**.** *Suppose that the nodes in $\mathcal{G}$ exchange information within an unknown radius R_n^{s}. Then, for the n^{th} and m^{th} node, if $\|p_n^{\mathrm{s}} - p_m^{\mathrm{s}}\| \leq R_n^{\mathrm{s}}$, we set $d(n, m) = 1$ and refer to the m^{th} node as a 1-hop neighbor of the n^{th} node. Subsequently, the set of $d(n, m)$-hop neighbors of the n^{th} node is $\mathcal{N}_n^{d(n,m)} = \{m \in \mathcal{V} : |\pi(n, m)| = d(n, m)\}$.*

As sensor networks are susceptible to various internal and external disturbances, some nodes may require maintenance during operation. This work aims to detect such nodes and, accordingly, formulates the central problem to be addressed.

Problem 1 (Detection of MRNs in sensor networks)**.** *An HSW of N sensors is deployed in a convex and compact region $\mathcal{Q} \subset \mathbb{R}^2$. These sensors have varying locations p_n^{s}, sensing ranges σ_n, and SI $g(q, p_n^{\mathrm{s}})$, rendering $\mathcal{Q}$ an uneven SI field. Then consider a team of I robots in $\mathcal{Q}$, with limited communication range R_c, detection range R_d and detection capability defined in* (2)*. They start from $P^{\mathrm{r}}(0)$ to search for MRNs and subsequently update their locations following* (1)*. Our goals are two-fold: (i) establish a criteria to define MRNs; (ii) synthesize a control strategy to detect MRNs.*

III. Hybrid Control Framework

Our framework for MRN detection adopts a two-stage hybrid control strategy that integrates SI-guided area exploration and NI-guided sensor detection. Specifically, the robots are guided by the SI of the HSN to search the space and identify high SI areas in the first stage, ensuring comprehensive coverage of the environment. In the second stage, individual robots perform local searches following the NI to locate the MRNs within the identified high SI areas. This design allows for efficient identification of MRNs while avoiding an exhaustive examination of nodes in the HSN. The overall framework is illustrated in Fig. 1.

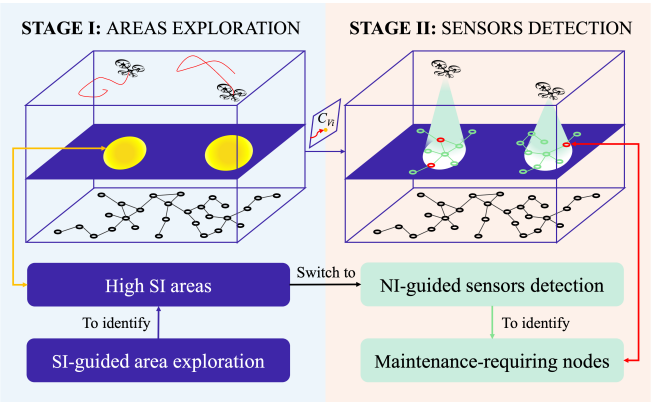

Fig. 1: Overview of the hybrid control framework.

A. Criteria for Maintenance Requesting Nodes

We establish criteria to identify MRNs that may severely damage the network communication when they become disconnected. We first introduce a probability to quantify the node's topological vulnerability, defined as follows:

$$\mathbb{P}(n) = \frac{|\Pi(n, \mathcal{N}_n^1)|}{\sum_{d(n,m)=1}^{N} |\Pi(n, \mathcal{N}_n^{d(n,m)})|}. \tag{3}$$

where $n, m \in \mathcal{V}$. Disconnection of a node isolates its one-hop neighbors and removes them from the HSN. Thus, this probability indicates the ratio between the communication path from the target node to its one-hop neighbors and the path from the target node to all communicable nodes within the HSN. This ratio directly reflects the number of isolated nodes resulting from node failure. Specifically, a higher ratio implies a greater dependence on the communication path between the node and its one-hop neighbors, leading to a higher number of isolated nodes upon failures. Conversely, a lower ratio indicates more indirect connections through multi-hop neighbors, which enhances the network robustness and reduces the number of isolated nodes after failures. For efficient real-time communication and computational feasibility, we consider nodes up to two hops away.

Notably, we exclude nodes located on the periphery of the network from analysis. These peripheral nodes exhibit weaker connections within the network topology, thus their disconnection has a marginal impact on the overall network functionality. Instead, we prioritize high SI areas to direct the robots towards more centrally located nodes. Consequently, we define the NI metric to evaluate the importance of nodes based on their connection strength and SI:

$$\mu(n) = \mathbb{P}(n)\phi(p_n^{\mathrm{s}}). \tag{4}$$

B. *Stage I:* Signal Intensity Guided Area Exploration

In stage I, we develop an SI-guided exploration strategy for robots to rapidly identify high SI areas, which potentially contain MRNs. The perceptual level of an individual robot toward a specific location is inversely correlated with the SI of that location; thus, a higher SI indicates a lower level of perception by the robot at that point. This mechanism naturally directs robots to prioritize movement toward high-SI areas, enhancing the system's spatial exploration efficiency.

For the RSs, we define the perceptual level on location q at time k by $\varphi(q,k)$, and the initial values are set as $\varphi(q,0) = \phi(q)$. To minimize ineffective exploration in areas with weak signals, we establish a lower threshold ϕ_0 for SI. Locations with SI values below ϕ_0 are considered fully known and do not require further exploration. Note that this threshold only applies to the initial perceptual level defined as:

$$\varphi(q,0) = \begin{cases} \phi(q) & \phi(q) \geq \phi_0, \\ 0 & \phi(q) < \phi_0. \end{cases} \tag{5}$$

Then, the update of a robot's perceptual level towards a specific point follows the dynamic equation below:

$$\varphi(q,k+1) = (1 - f(q, p_i^{\mathrm{r}}(k)))\varphi(q,k). \tag{6}$$

We set its increment as $\Delta\varphi(q,k) = -f(q,p_i^{\mathrm{r}}(k))\varphi(q,k)$. Given that $\varphi(q,k)$ is a decreasing function, $\Delta\varphi(q,k)$ is thus negative. Based on this, our objective is to maximize the magnitude of the change between two moments, represented as $\min \Delta\varphi(q,k)$. Therefore, the objective of this section is to maximize the following function within the global scope of the tasks area composed of Voronoi cells:

$$\mathcal{H}(P^{\mathrm{r}}(k),k) = \int_{\mathcal{Q}} f(q, p_i^{\mathrm{r}}(k))\varphi(q,k)dq. \tag{7}$$

To ensure the orderly operation of the RS within the task environment, it is essential to establish clear dominance for each robot. We apply Voronoi tessellation to partition the area into distinct domains for each robot as follows:

$$V_i(k) = \{q \in \mathcal{Q} \mid \|q - p_i^{\mathrm{r}}(k)\| \leq \left\|q - p_j^{\mathrm{r}}(k)\right\|, \forall j \neq i\}. \tag{8}$$

By optimizing locational costs, we enhance the coordination among the robots. Then, a gradient-based approach is utilized to maximize the cost function [22], *i.e.*, $\max \mathcal{H}(P^{\mathrm{r}}(k),k)$, can be derived as follows:

$$\begin{aligned} \frac{\partial \mathcal{H}(P^{\mathrm{r}}(k),k)}{\partial p_i^{\mathrm{r}}(k)} &= \int_{V_i(k)} \frac{\partial f(q, p_i^{\mathrm{r}}(k))}{\partial p_i^{\mathrm{r}}(k)} \varphi(q,k)dq \\ &= M_{V_i}(p_i^{\mathrm{r}}(k) - C_{V_i}), \end{aligned} \tag{9}$$

where M_{V_i} and C_{V_i} respectively represent the mass and centroid within $V_i(k)$, as shown below:

$$M_{V_i} = \int_{V_i(k)} 2\delta\lambda e^{-\lambda\|q - p_i^{\mathrm{r}}(k)\|^2} \varphi(q,k)dq, \tag{10}$$

$$C_{V_i} = \frac{1}{M_{V_i}} \int_{V_i(k)} 2\delta\lambda e^{-\lambda\|q - p_i^{\mathrm{r}}(k)\|^2} \varphi(q,k) q dq. \tag{11}$$

Therefore, the control law is expressed as:

$$u_i^{\mathrm{si}}(k) = -\kappa^{\mathrm{si}}(p_i^{\mathrm{r}}(k) - C_{V_i}). \tag{12}$$

Note that the control strategy comprises two independent stages. To enable the timely initiation of the second stage, the SI-guided area exploration must be completed within a finite time. This requirement is formalized in Theorem 1.

Theorem 1. *The SI-guided area exploration stage completes in a finite time.*

To analyze the performance of our control law on RS, we establish Theorem 2 for the area exploration process:

Theorem 2. *Under the control law* (12)*, the trajectories taken by RS, from any initial configuration* $P^{\mathrm{r}}(0)$*, invariably converge to the critical points of* $\mathcal{H}$*.*

During this stage, the robots asymptotically converge to the centroids of their respective Voronoi cells, thus moving towards high-SI regions that potentially require investigation. This also ensures efficient spatial distribution of the RS.

C. *Stage II:* Node Influence Guided Sensors Detection

Following the first stage, the i^{th} robot disperses towards the centroid of the area with high SI, meanwhile employs its onboard equipment to detect nodes within the range R_d that are subsequently added to the set $D_i(k) = \{n \in \mathcal{V} : \|p_n^{\mathrm{s}} - p_i^{\mathrm{r}}(k)\| \leq R_d\} \cap V_i(k)$. The second detection process aims to pinpoint the MRNs within $D_i(k)$.

Within its autonomous domain, the i^{th} robot calculates $\max_{n\in D_i(k)} \mu(n)$, however, attains only a local optimum. This is attributed to the fact that the maximum value identified by a robot within its designated area is not guaranteed to be the maximum value in another robot's autonomous region, indicating that local optima do not necessarily correspond to global optima. This situation is exemplified by $\mu(m) > \max_{n\in D_i(k)} \mu(n)$, where $m \in D_j(k)$. For global optimization, we set the influence threshold θ of the HSN as:

$$\theta = \min_{i\in\{1,\ldots,I\}} \max_{n\in D_i(k)} \mu(n). \tag{13}$$

Nodes with NI values larger than the threshold are identified as MRNs, which are then included in the set $M_i = \{n \in D_i(k) : \mu(n) > \theta\}$. The i^{th} robot computes the barycenter of the MRNs within M_i as in (14) and moves towards B_{M_i} to monitor vulnerable nodes for potential maintenance.

$$B_{M_i} = \frac{1}{|M_i|} \sum_{n\in M_i} p_n^{\mathrm{s}}. \tag{14}$$

The control law for this stage is defined as:

$$u_i^{\mathrm{ni}}(k) = -\kappa^{\mathrm{ni}}(p_i^{\mathrm{r}}(k) - B_{M_i}), \tag{15}$$

where $\kappa^{\mathrm{ni}} = v\,\|p_i^{\mathrm{r}}(k) - B_{M_i}\|^{-1}$.

The MRNs detection based on NI can be considered as sorting several nodes, which determines the worst bound of finite-time convergence k. For example, bubble sort exhibits $O(n^2)$ time complexity, while merge sort operates at $O(n \log n)$. Using bubble sorting as an example, identifying the maximum NI value among n nodes at time k requires, in the worst-case scenario, comparisons. $n(n-1)/2$. Extending this to selecting minimum NI values across I robots incurs $I(I-1)/2$ comparisons in the most unfavorable case, which can also guarantee task completion within a finite time. This result is formally presented in the following theorem:

Theorem 3. *The whole hybrid control procedure is completed in a finite time.*

This result ensures that the entire hybrid control process—from initial SI-guided exploration to final node detection—terminates within a bounded time, which is essential for practical deployment in large-scale sensor networks with time-sensitive maintenance needs. Furthermore, we assess the convergence properties of the NI-guided control law to ensure the reliability of node localization.

Theorem 4. *Under the control law* (15)*, the trajectory of the* i^{th} *robot is asymptotically stable and converges to* B_{M_i}*.*

This result implies that each robot, upon entering the NI-guided detection stage, converges to the barycenter of nearby MRNs. This stable behavior enables efficient localization of critical nodes. Due to space limitations, a proof is omitted here but will be provided in a forthcoming extended version.

D. Hybrid Control Law

We have implemented a hybrid control framework to facilitate the integration of the two stages and define the conditions for task completion. We start by defining the error of the i^{th} robot at moment k in the two following processes:

$$\begin{aligned} |e_i^{\mathrm{si}}(k)| &= |p_i^{\mathrm{r}}(k) - C_{V_i}|, \\ |e_i^{\mathrm{ni}}(k)| &= |p_i^{\mathrm{r}}(k) - B_{M_i}|. \end{aligned} \tag{16}$$

To ensure that the control strategy permanently switches from stage I to stage II, we define a flag $\Gamma_i(k)$ governed by:

$$\Gamma_i(k+1) = \begin{cases} 1, & \text{if } \Gamma_i(k) = 0 \text{ and } |e_i^{\mathrm{si}}(k)| \leq \epsilon^{\mathrm{si}}, \\ \Gamma_i(k), & \text{otherwise.} \end{cases} \tag{17}$$

Initially, $\Gamma_i(0) = 0$. Once the SI error $|e_i^{\mathrm{si}}(k)|$ falls below the threshold ϵ^{si}, the control law switches to $u_i^{\mathrm{ni}}(k)$ and remains there thereafter, which is formally stated as:

$$u_i(k) = \begin{cases} u_i^{\mathrm{si}}(k), & \text{if } \Gamma_i(k) = 0, \\ u_i^{\mathrm{ni}}(k), & \text{if } \Gamma_i(k) = 1. \end{cases} \tag{18}$$

The detection process terminates when $|e_i^{\mathrm{ni}}(k)| \leq \epsilon^{\mathrm{ni}}$ holds, indicating that the robot has effectively approached the barycenter of the identified MRNs. In particular, the proposed hybrid control law (18) incorporates a rigorously designed switching flag (17) to govern transitions between control modes. This mechanism ensures that, once the predefined switching condition is met, the system irreversibly transitions from the control law (12) to (15). This one-way transition effectively eliminates the possibility of Zeno behavior—characterized by an infinite number of control switches in a finite time—which often undermines the stability of hybrid systems. By enforcing this irreversible switching logic, the framework guarantees finite-time convergence and ensures that control actions remain implementable.

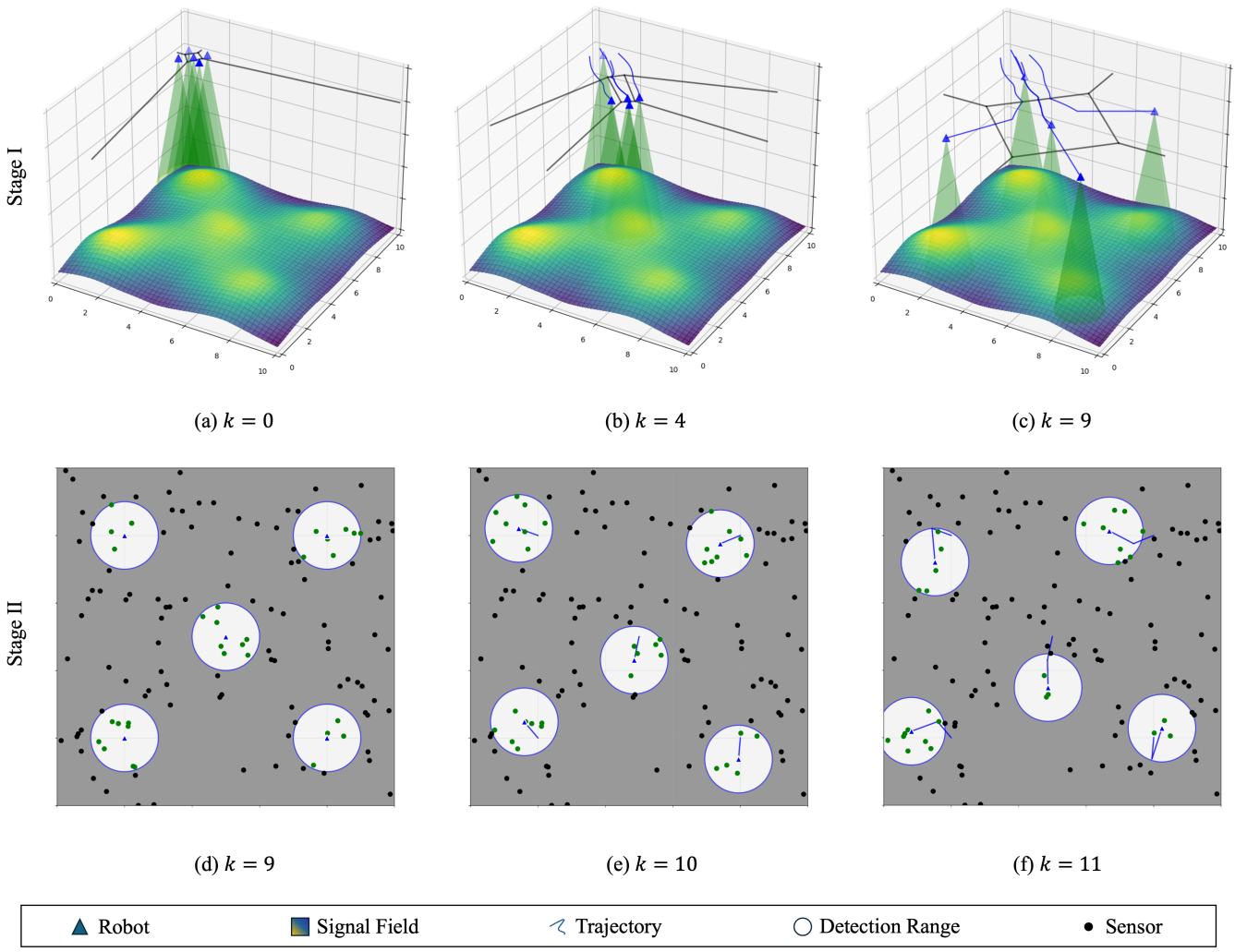

Fig. 2: The deployment of the robot swarm executing the proposed hybrid control framework.

IV. Simulation Results

This section provides simulation results to validate that our hybrid control approach is effective in exploring the deployed area of robot swarms and detecting the structurally vulnerable nodes in an HSN. To this end, we consider a square operational area $\mathcal{Q}$, each side measuring 10km. Our simulation environment is discretized as a grid of resolution $x = y = 0.002$km, and the simulation is conducted in discrete time with a sampling period $T_s = 1$min.

In this task area, 150 nodes are randomly distributed. These nodes are segmented into five clusters, each comprising 30 nodes, and assigned distinct communication radii of 0.5km, 0.75km, 1km, 1.25km, and 1.5km, respectively. The SI among nodes adheres to the function $\phi(q, 0)$, defined by the parameters $\gamma_z = 0.5 + 0.25z$ and $\sigma_z = 2 + z$, with the cluster index $z = 0, 1, 2, 3, 4$.

The RS comprises 5 robots, each with initialized positions within the defined bounded area. These robots are equipped with a communication radius of $R_c = 4$km and a detection radius of $R_d = 1$km and are programmed to achieve a maximum forward velocity of $v = 72$km/h. The sensing capabilities of these robots are delineated by the equation (2), with parameters $\delta = 1$ and $\lambda = 0.02$. Furthermore, we have configured the control law gains at $\kappa^{\text{si}} = 0.6$ and $\kappa^{\text{ni}} = 1$, while establishing an acceptable error margin delineated by $\epsilon^{\text{si}} = 0.002$km and $\epsilon^{\text{ni}} = 0.002$km.

We start by implementing the control law (18). The subfigures (a)∼(c) depict the trajectories of robots guided by the SI field toward the centroids of their respective Voronoi cells in Fig. 2. The background color in the simulation visually indicates the level of perception that the robots have of a specific area: blue signifies low SI, denoting a high perception level of the area by the robot, whereas yellow indicates high SI, meaning a lower perception level of the area. The subfigures (i)∼(l) depict the navigation process based on NI, which drives the robots towards the barycenters of their associated MRNs. In terms of trajectory characteristics, stage I features smooth trajectories, while stage II involves piecewise-linear trajectories. The integration of these two distinct trajectory types exemplifies the hybrid nature of the proposed method.

We proceed to evaluate the performance of the proposed method. The assessment relies on the error metric defined in (16), with the corresponding results illustrated in Fig. 3. The switching flag delineates the control process into two distinct stages, each characterized by a monotonic decrease in the error metric. This consistent decline not only confirms the convergence properties of the approach but also substantiates its effectiveness across distinct control regimes.

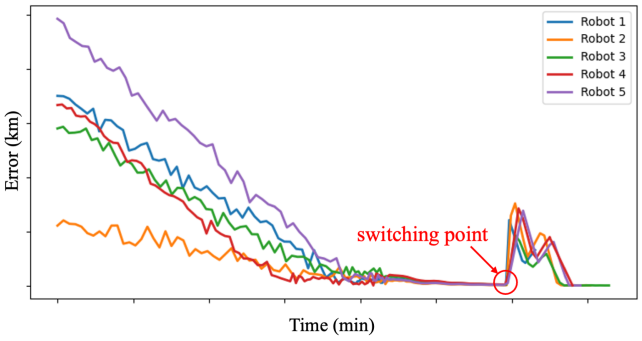

Fig. 3: Performance of the RS's tracking error.

To further contextualize its performance, we conducted comparative analyses with both the centroidal voronoi tessellation (CVT) [22] and exhaustive search (ES) algorithms. When relying solely on CVT for MRN detection, the control procedure tends to terminate prematurely, often failing to accurately localize the MRNs. In contrast, the ES requires robots to inspect all nodes. While this method guarantees completeness, its efficiency is highly sensitive to the initial spatial distribution of the robots. In an ideal setting—where five robots each inspect 30 nodes—the full detection process can theoretically be completed within 31min. We conducted 100 simulations under varying HSW topologies and randomized initial configurations of the RS position. A statistically significant result is summarized in TABLE I.

TABLE I: Comparison of performance of various strategies.

Index	this paper	CVT	ES
End time	11.02min	10.85min	88.47min
Detection efficiency	9.07	9.22	1.69
Accuracy ratio	100%	48.67%	100%

V. Conclusion

In this work, we developed a novel hybrid control framework that integrates area exploration and node detection to efficiently identify structural vulnerability in HSNs. We began by designing a coverage control strategy based on the sensing capacity of the robots and the distribution of the HSN's signal intensity. Then, we defined a node influence metric and proposed a barycenter-driven control method for node detection based on the index. Finally, we conducted empirical studies to demonstrate the performance of the method. For further research, we will extend our framework to consider time-varying sensor networks and heterogeneous robot swarms with different sensing and control capabilities, where distributed control is essential.

References

[1] A. T. Farhad Samadzadegan and F. D. Javan, "A critical review on multi-sensor and multi-platform remote sensing data fusion approaches: current status and prospects," *International Journal of Remote Sensing*, vol. 46, no. 3, pp. 1327–1402, 2025.

[2] D. J. Yeong, G. Velasco-Hernandez, J. Barry, and J. Walsh, "Sensor and sensor fusion technology in autonomous vehicles: A review," *Sensors*, vol. 21, no. 6, 2021.

[3] A. Torreño, E. Onaindia, A. Komenda, and M. Štolba, "Cooperative multi-agent planning: A survey," *ACM Computing Surveys*, vol. 50, no. 6, 2017.

[4] N. Hossein Motlagh, P. Kortoçi, X. Su, L. Lovén, H. K. Hoel, S. Bjerkestrand Haugsvær, V. Srivastava, C. F. Gulbrandsen, P. Nurmi, and S. Tarkoma, "Unmanned aerial vehicles for air pollution monitoring: A survey," *IEEE Internet of Things Journal*, vol. 10, no. 24, pp. 21687–21704, 2023.

[5] Z. Wang, Y. Zhang, C. Zhao, and H. Yu, "Adaptive event-triggered formation control of autonomous vehicles," *arXiv preprint arXiv:2506.06746*, 2025.

[6] A. d. S. Batista and A. L. Dos Santos, "A survey on resilience in information sharing on networks: Taxonomy and applied techniques," *ACM Computing Surveys*, vol. 56, Oct. 2024.

[7] G. T. L. da F. Costa, F. A. Rodrigues and P. R. V. Boas, "Characterization of complex networks: A survey of measurements," *Advances in Physics*, vol. 56, no. 1, pp. 167–242, 2007.

[8] M. E. Newman, "The structure and function of complex networks," *SIAM review*, vol. 45, no. 2, pp. 167–256, 2003.

[9] H.-N. Dai, R. C.-W. Wong, H. Wang, Z. Zheng, and A. V. Vasilakos, "Big data analytics for large-scale wireless networks: Challenges and opportunities," *ACM Computing Surveys*, vol. 52, no. 5, pp. 1–36, 2019.

[10] M. Minelli, J. Panerati, M. Kaufmann, C. Ghedini, G. Beltrame, and L. Sabattini, "Self-optimization of resilient topologies for fallible multi-robots," *Robotics and Auto. Systems*, vol. 124, p. 103384, 2020.

[11] H. Kabir, M.-L. Tham, and Y. C. Chang, "Internet of robotic things for mobile robots: Concepts, technologies, challenges, applications, and future directions," *Digital Communications and Networks*, vol. 9, no. 6, pp. 1265–1290, 2023.

[12] S. J. Chung, A. A. Paranjape, P. Dames, S. Shen, and V. Kumar, "A survey on aerial swarm robotics," *IEEE Transactions on Robotics*, vol. 34, no. 4, pp. 837–855, 2018.

[13] M. Santos, Y. Diaz-Mercado, and M. Egerstedt, "Coverage control for multirobot teams with heterogeneous sensing capabilities," *IEEE Robotics and Automation Letters*, vol. 3, no. 2, pp. 919–925, 2018.

[14] G. Sun, R. Zhou, Z. Ma, Y. Li, R. Groß, Z. Chen, and S. Zhao, "Mean-shift exploration in shape assembly of robot swarms," *Nature Communications*, vol. 14, no. 1, p. 3476, 2023.

[15] Y. Bai, P. T. Tran Ngoc, H. D. Nguyen, D. L. Le, Q. H. Ha, K. Kai, Y. X. See To, Y. Deng, J. Song, N. Wakamiya, *et al.*, "Swarm navigation of cyborg-insects in unknown obstructed soft terrain," *Nature Communications*, vol. 16, no. 1, p. 221, 2025.

[16] S. Sundaram and B. Gharesifard, "Distributed optimization under adversarial nodes," *IEEE Transactions on Automatic Control*, vol. 64, no. 3, pp. 1063–1076, 2018.

[17] Y. Gao, K. Luo, C. Fang, and J. He, "Fragility-aware stealthy attack strategy for multi-robot systems against multi-hop wireless networks," in *IEEE 61st Conf. on Decision and Control*, pp. 4827–4832, 2022.

[18] L. Zhang, Z. Zhang, R. Siegwart, and J. J. Chung, "Distributed PDOP coverage control: Providing large-scale positioning service using a multi-robot system," *IEEE Robotics and Automation Letters*, vol. 6, no. 2, pp. 2217–2224, 2021.

[19] K. Nakamura, M. Santos, and N. E. Leonard, "Decentralized learning with limited communications for multi-robot coverage of unknown spatial fields," in *IEEE/RSJ International Conference on Intelligent Robots and Systems (IROS)*, pp. 9980–9986, 2022.

[20] S. Haddadin, A. De Luca, and A. Albu-Schäffer, "Robot collisions: A survey on detection, isolation, and identification," *IEEE Transactions on Robotics*, vol. 33, no. 6, pp. 1292–1312, 2017.

[21] L. Siligardi, J. Panerati, M. Kaufmann, M. Minelli, C. Ghedini, G. Beltrame, and L. Sabattini, "Robust area coverage with connectivity maintenance," in *International Conference on Robotics and Automation (ICRA)*, pp. 2202–2208, 2019.

[22] J. Cortes, S. Martinez, T. Karatas, and F. Bullo, "Coverage control for mobile sensing networks," *IEEE Transactions on robotics and Automation*, vol. 20, no. 2, pp. 243–255, 2004.